Numerical simulation of a turbulent methanol spray flame using the Euler-Lagrange method and the steady laminar flamelet model

Shanglong Zhu *, Dirk Roekaerts ** and Theo van der Meer *
s.zhu@utwente.nl
*Laboratory of Thermal Engineering, University of Twente, the Netherlands
**Department of Multi-scale Physics, Delft University of Technology, the Netherlands

Abstract
The modeling and simulation of the turbulent spray combustion is necessary for a better understanding of the characteristics of the turbulent spray combustion in detail. However, many complex processes are involved and strongly coupled which makes the validation of the simulation essential. Light oils are often used in the experiment for the validation because their properties and detailed chemistry have been investigated repeatedly and are readily available. In the present study, a methanol spray flame in a chamber of the NIST was modeled in ANSYS Fluent, and the results were compared and validated by the experimental data. Features of this flame, including the boundary conditions of the inlet air and the spray, were analyzed according to the experiment. The standard k-ε model with the enhanced wall treatment and the Euler-Lagrange method were employed for the simulation of the turbulence and spray. The predicted mean velocity components of the air flow at various downstream elevations showed good agreements with the experiment. The steady laminar flamelet model was employed in order to include detailed chemical reactions without a considerable increase in computational time. The droplet number density, SMD, and the mean axial and radial velocities of the droplets were compared to the measured data. In addition, the influence of the source term of the mixture fraction variance due to evaporation was investigated in this case. The results showed that although the source term had influence on the calculation in the lower part of the flame, where the peak mean mixture fraction variance increased from 0.013 to 0.016, the combustion characteristics did not change much with the peak temperature increasing within 10K.

1.Introduction
Turbulent spray combustion systems are widely utilized in industry boilers, internal combustion engines, and gas turbines. The combustion efficiency, stability, and pollutant formation strongly depend on the characteristics of the turbulent spray combustion, and a better understanding of the turbulent spray combustion is required.
The numerical simulation of the turbulent spray combustion is considered to be an easier and safer way to understand the characteristics of combustion in detail rather than the experiment. However, the modeling and simulation of the turbulent spray is particularly challenging because complex processes involving turbulence, atomization, evaporation, combustion and radiative heat transfer are included and they are strongly coupled. To improve the reliability of the spray combustion simulation, it is necessary to compare the prediction with experimental data and to test how the mathematical models perform.
Light oils are often used in the experiment for the validation because their properties and detailed chemistry have been investigated repeatedly and are readily available. It is necessary to include the detailed chemistry for the simulation especially with ignition and extinction processes, as well as the pollutant formation. However, due to the strong coupling between the equations with considerable change of density for the turbulent spray combustion, the calculation with volumetric reactions like the Eddy Dissipation Concept (EDC) model

proposed by Magnussen [1], which is widely used in gaseous combustion, does not converge well with the detailed chemistry.

The laminar flamelet method provides a feasible way to include detailed chemical reactions in turbulent combustion simulations without a considerable increase in computational time. It assumes that in the gaseous phase combustion, the diffusion coefficients for all species are equal, and then the species mass fraction and temperature are mapped from physical space to mixture fraction space and can be uniquely described by two parameters: the mixture fraction ξ and the scalar dissipation χ. The Favre-averaged values of quantities in the turbulent flame are then obtained through the use of Favre-averaged probability density function, $\tilde{f}(\xi,\chi)$:

$$\tilde{\Phi} = \int_0^\infty \int_0^1 \Phi(\xi,\chi)\tilde{f}(\xi,\chi)d\xi d\chi \tag{1}$$

Hence, the complex chemistry can be reduced to two variables and allows the flamelet calculations to be preprocessed and tabulated, offering tremendous computational savings.

In the present paper, the reported turbulent methanol spray flame carried out by John F. Widmann and Cary Presser [2] at the National Institute of Standards and Technology (NIST) is simulated in ANSYS Fluent with the steady laminar flamelet model. The interaction processes between droplets and continuous phase are simulated by use of Dispersed Phase model with the Linearized Instability Sheet Atomization (LISA) model of Schmidt et al. [3]. Previous simulations [4,5,6] and the features of this flame, including the boundary conditions of the inlet air and the spray, are analyzed to relate the experiment and simulations. Predictions of the mean velocity components of air flow and droplets, droplet number density, and Sauter Mean Diameter (SMD) are compared with the experimental data. Furthermore, the influence of the evaporation on mixture fraction variance is investigated.

2.Experiment and boundary conditions

The NIST flame experiment was carried out in a combustion chamber, shown in Figure 1. Swirling combustion air generated by a movable 12-vane swirl cascade passes through the outer annulus passage. A pressure-jet nozzle forms a hollow-cone methanol spray with a nominal 60° full cone angle from the inner circular port. The inlet conditions are shown in Table 1.

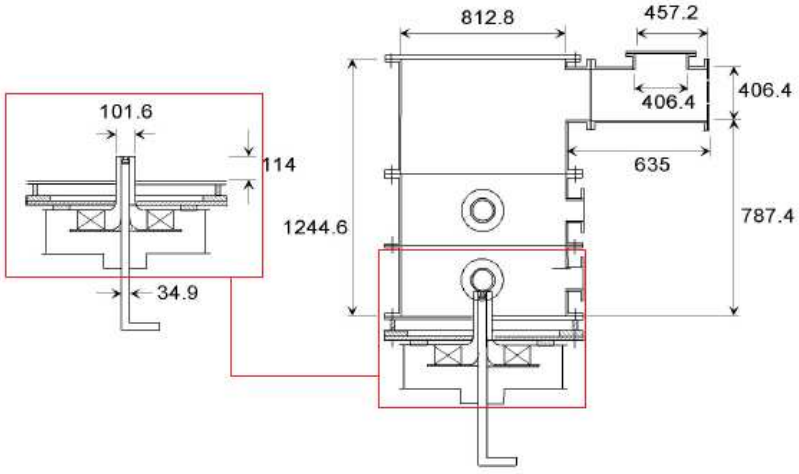

Figure 1. Setup and dimensions (mm) of the NIST flame experiment.

As Cary Presser [7] highlighted in the analysis of this experiment, the accurate representation of the boundary conditions is essential to carrying out a successful simulation, the description

of the inlet co-flow, heat transfer and the spray for the modeling requires to be well defined in prior.

Table 1. Inlet conditions of air and fuel.

Air flow rate (m3/h)	56.7±1.7 [a]
Air temperature (K)	298
Fuel flow rate (kg/h)	3.0±0.02
Fuel temperature (K)	298
Injection pressure (Pa)	690000
Spray angle	60°

a: interpolated data within relative error of 5% is used in the simulation.

As for the air inlet conditions, the air velocity components at downstream elevation z=1.4mm near the air inlet both with and without the spray are measured in the experiment. Based on the previous simulations and analysis, the velocity components at this elevation can represent the inlet conditions, and the data measured when the spray is present are supposed to be a better assumption for the simulation of the spray combustion.

For the walls, a convection coefficient with the ambient of 12 $Wm^{-2}K^{-1}$ and a surrounding ambient temperature of 298 K also used in J.Collazo's work [5] are adopted.

With regard to the spray, besides the inlet conditions of the fuel shown in Table 1, the injector exit diameter and the parameters for the droplet diameter distribution required in the spray model are not clear and we have to deduce them from the experimental data.

The droplet number density at seven axial locations downstream of the nozzle exit (z = 5, 15, 25, 35, 45, 55, and 65 mm) from the experiment [2] are then analyzed to estimate the injector exit diameter, as shown in Figure 2.

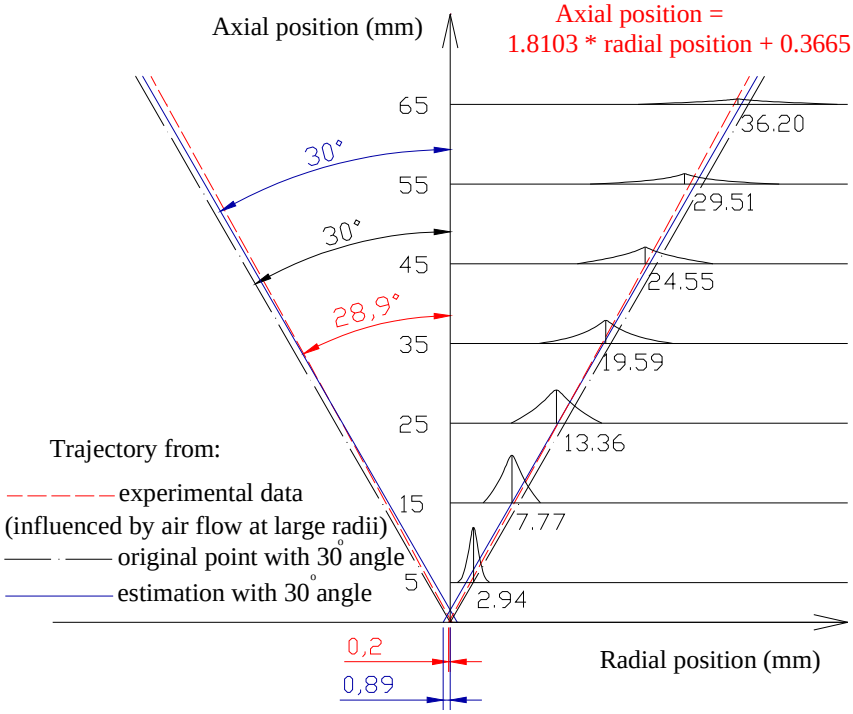

Figure 2. Estimation of the radial location of the spray.

As a result, the injector exit diameter is estimated to be about 1.78 mm. Furthermore, the influence of the dispersion angle, sheet constant and ligament constant on the predicted results

were investigated, and a combination of a dispersion angle of 10°, a sheet constant of 12 and a ligament constant of 0.5 was employed in our simulations for the spray model.

3.Mathematical model

3.1. Grid and turbulence model

Convincing demonstration of grid independence is essential for reliable simulations and must be shown. However, grid independence in full 3D simulations is more difficult to be validated than in 2D simulations because of both complexity and computational cost, especially when there is a swirl and hybrid grids are employed.

For the simulation of the NIST flame, it was concluded through a 3D CFD study of the experiment by Crocker et al. [4] that the influence of the exhaust channel on the simulation of the near-nozzle region was negligible and that it could be omitted in the geometry, considering the end of the combustion chamber as open boundary. As a result, the 2D axisymmetric swirl simulation is employed in the present study. It simplifies the 3D case into a 2D case with circular cylindrical coordinates.

The grid independence was then tested by introducing a series of different element sizes with the same aspect ratio of 3. The role of the near-wall treatment for this swirling flow was analyzed. As a result a 2D mesh with about 46000 quadrilateral cells and the second order upwind scheme were found suitable for this study. A standard k-ε turbulence model with the enhanced wall treatment is employed based on the comparative analysis.

3.2. Spray model

The atomization process of light oil sprays is commonly modeled using a wave growth or aerodynamic theory that predicts spray parameters such as the spray angle and the drop diameter. The surface wave instability model proposed by Reitz, the Kelvin-Helmholtz/Rayleigh-Taylor (KHRT) Instability model by Patterson and Reitz and the Taylor Analogy Breakup (TAB) model by O'Rourke and Amsden are widely used atomization models. However, the coupling with the nozzle effects and the primary atomization is largely unknown and is usually represented by an arbitrary nozzle-dependent constant.

For the pressure swirl atomizer in the NIST flame, we employ the LISA model. It assumes that Kelvin-Helmholtz waves grow on the sheet and eventually break the liquid into ligaments. It is then assumed that the ligaments break up into droplets due to varicose instability. Once the liquid droplets are formed, the spray evolution is determined by drag, collision, coalescence, and secondary breakup.

For film formation, the relationship between the thickness of this film, t, and the mass flow rate is as follows:

$$\dot{m}_{eff} = \pi \rho u t (d_{inj} - t) \tag{1}$$

where d_{inj} is the injector exit diameter, $\dot{m}_{eff}$ is the effective mass flow rate, and u is the axial component of velocity at the injector exit. Because u depends on internal details of the injector and is difficult to calculate from first principles, the approach of Han et al. [8] is used and the total velocity is assumed to be related to the injector pressure by:

$$U = k_v \sqrt{\frac{2\Delta P}{\rho_l}} \tag{2}$$

where k_v is the velocity coefficient and a function of the injector design and injection pressure [9]. If ΔP is known, u can be calculated as

$$u = U \cos\theta \tag{3}$$

where θ is the spray angle.

For sheet breakup and atomization, the pressure-swirl atomizer model includes the effects of the surrounding gas, liquid viscosity and surface tension on the breakup of the liquid sheet. It is based upon the growth of sinuous waves on the liquid sheet. For waves that are long compared with the sheet thickness, ligaments are assumed to form from the sheet breakup process once the unstable waves reach critical amplitude. If the surface disturbance has reached a value of η_b at a breakup time τ, the sheet breaks up and ligaments will be formed at a length given by:

$$L_b = U_\tau = \frac{U}{\Omega}\ln(\frac{\eta_b}{\eta_O}) \tag{4}$$

where Ω is the maximum growth rate, and $\ln(\eta_b / \eta_O)$ is an empirical sheet constant. The default value of 12 was obtained theoretically by Weber [10] for liquid jets. Dombrowski and Hooper [11] showed that a value of 12 for the sheet constant agreed favorably with experimental sheet breakup lengths over a range of Weber numbers from 2 to 200.

Thus the diameter of the ligaments formed at the point of breakup can be obtained from a mass balance:

$$d_L = \sqrt{\frac{8h}{K_S}} \tag{5}$$

where K_S is the wave number corresponding to the maximum growth rate, and the film thickness can be calculated from the breakup length and the radial distance from the centre line to the mid-line of the sheet at the atomizer exit r_0:

$$h_{end} = \frac{r_0 h_0}{r_0 + L_b \sin(\frac{\theta}{2})} \tag{6}$$

For waves that are short compared to the sheet thickness, the ligament diameter is assumed to be linearly proportional to the wavelength that breaks up the sheet:

$$d_L = \frac{2\pi C_L}{K_S} \tag{7}$$

where C_L is the ligament constant and equal to 0.5 by default.

In either the long-wave or the short-wave case, the breakup from ligaments to droplets is assumed to behave according to Weber's [10] analysis for capillary instability. So the most probable diameter for droplet diameter distribution, d_0, is determined from:

$$d_0 = 1.88 d_L (1 + 3Oh)^{1/6} \tag{8}$$

where Oh is the Ohnesorge number which is a combination of the Reynolds number and the Weber number.

Once this most probable droplet size of a Rosin-Rammler distribution has been determined, with a spread parameter of 3.5 and a default dispersion angle of 6° which are based on past modeling experience [12], the droplet diameter distribution is determined.

In the simulation, the fuel is assumed to be injected into the chamber as a fully atomized spray consisting of spherical droplets of various sizes. The motions of the droplets in the turbulent combustion flow field are calculated using a stochastic tracking method so that the momentum, mass, and energy exchange between the droplets and the gas phase can be simulated by tracking a large number of droplets.

The equation of motion for a droplet is represented as:

$$\frac{du_{p,i}}{dt} = \frac{18\mu}{\rho_p D_p^2}\frac{C_D \,\mathrm{Re}}{24}(U_i - u_{p,i}) + \frac{g_i(\rho_p - \rho)}{\rho_P} + F_i \tag{9}$$

In this equation, u_P is the particle velocity, U is a sampled gas velocity, μ is the molecular viscosity of the fluid, ρ_p is the fluid density, ρ is the density of the particle, D_P is the particle diameter, Re is the relative Reynolds number and the drag coefficient C_D is a function of the particle Reynolds number. F_i is an additional acceleration term.

As for secondary breakup, the Taylor analogy breakup (TAB) model, which is based upon Taylor's analogy [13] between an oscillating and distorting droplet and a spring mass system, is employed in the simulation of the NIST flame, since this case has low-Weber-number injections and the TAB model is well suited for low-speed sprays into a standard atmosphere.

For droplet collision and coalescence, the algorithm of O'Rourke [14] is employed. It uses the concept of a collision volume to calculate the probability of collision. In general, once two parcels are supposed to collide, the outcome tends to be coalescence if the droplets collide head-on, and bouncing if the collision is more oblique. The probability of coalescence can be related to the offset of the collector droplet centre and the trajectory of the smaller droplet. The critical offset is a function of the collisional Weber number and the relative radii of the collector and the smaller droplet.

The rate of vaporization is governed by gradient diffusion, with the flux of droplet vapor into the gas phase related to the difference in vapor concentration at the droplet surface and the bulk gas:

$$N_i = k_c(C_{i,s} - C_{i,\infty}) \tag{10}$$

where N_i represents the molar flux of vapor, k_c the mass transfer coefficient, $C_{i,s}$ the vapor concentration at the droplet surface, and $C_{i,\infty}$ the vapor concentration in the bulk gas. The concentration of vapor at the droplet surface is evaluated by assuming that the partial pressure of vapor at the interface is equal to the saturated vapor pressure, p_{sat}, at the particle droplet temperature, T_p:

$$c_{i,s} = \frac{p_{sat}(T_p)}{RT_p} \tag{11}$$

where R is the universal gas constant.

3.3. Radiative heat transfer and combustion model

According to the analysis of the NIST flame, radiative heat transfer can not be neglected in the simulation of the NIST flame. The Discrete Ordinates (DO) radiation model with a variable absorption coefficient, the weighted-sum-of-gray-gases model (WSGGM), is employed.

The detailed reaction mechanism for methanol employed in the present study was developed by R.P. Lindstedt and M.P [15] and provided by Peter Lindstedt and J-Y Chen with a chemkin compatible reduced mechanism. It comprises 32 species and 167 reactions.

Because of the relative fast chemistry of methanol, the steady laminar flamelet model is used here and the flame is assumed to respond instantaneously to the aerodynamic strain. Additionally, the heat gain/loss to the system is assumed to have a negligible effect on the species mass fractions and adiabatic mass fractions are used [16,17]. The flamelet profiles are then convoluted with the assumed β-shape PDFs as in Equation (1), and then tabulated for look-up. Figure 3 shows a schematic structure of the preprocessed look-up table in the present study. The equations for the mean mixture fraction, mixture fraction variance, and mean enthalpy are solved. The scalar dissipation field is calculated from the turbulence field and the mixture fraction variance as follows:

$$\tilde{\chi} = \frac{C_\chi \tilde{\varepsilon} \tilde{\xi}''^2}{\tilde{k}} \tag{12}$$

where C_χ is set to the standard value 2.

The mean values of cell temperature, density, and species mass fraction are obtained from the PDF look-up table.

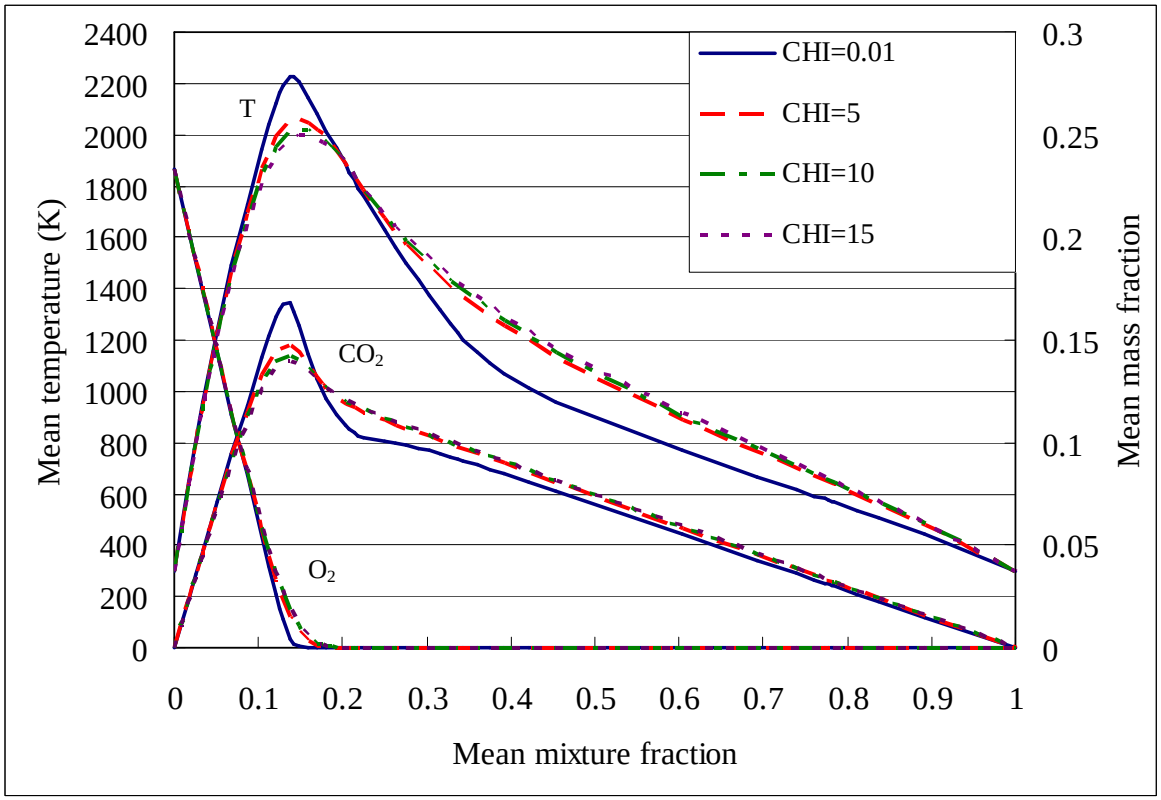

Figure 3. A schematic structure of the preprocessed look-up table in the present study

Furthermore, in order to investigate the influence of a source term due to evaporation in the mixture fraction variance equation, $\bar{\dot{\rho}}_s \tilde{\xi}''^2 (1-2\tilde{\xi})\tilde{\xi}$, see [18], calculations were made without and with this source terms included.

4.Results and Discussion

Between the results with and without the source term in the mixture fraction variance, no considerable difference of the air flow and droplets is observed. The predicted mean velocity components at different downstream elevations compared with experiment are shown in Figure 4. The bar at each point of the experimental data represents the uncertainty of the measurement.

At large radii ($>$17.45mm), where the air flow, instead of the spray, dominates the flow field, the results resemble the experimental data well. The deviations at large radii for the tangential velocity at z=9.5mm and z=17.6mm looks like considerable. However, if we take into account the influence of the considerable uncertainties of the data at z=1.4mm, which are considered as the inlet condition, the deviations are still minor. When it goes to the small radii, deviations against the experimental data for axial and radial velocities can be observed. This is also reported in other research [5,6]. One explanation is that the interaction between the droplets and the continuous phase is overestimated. However, because the acceleration of the continuous phase by the spray and thermal expansion of the continuous phase do result in the higher velocity components, an alternative more reasonable explanation is that it is difficult to

measure velocity components of a gaseous phase in a region where a dispersed phase is present in high concentration. For the tangential velocity, the predicted results at small radii resemble the experiment well because the tangential velocity is not accelerated by the spray.

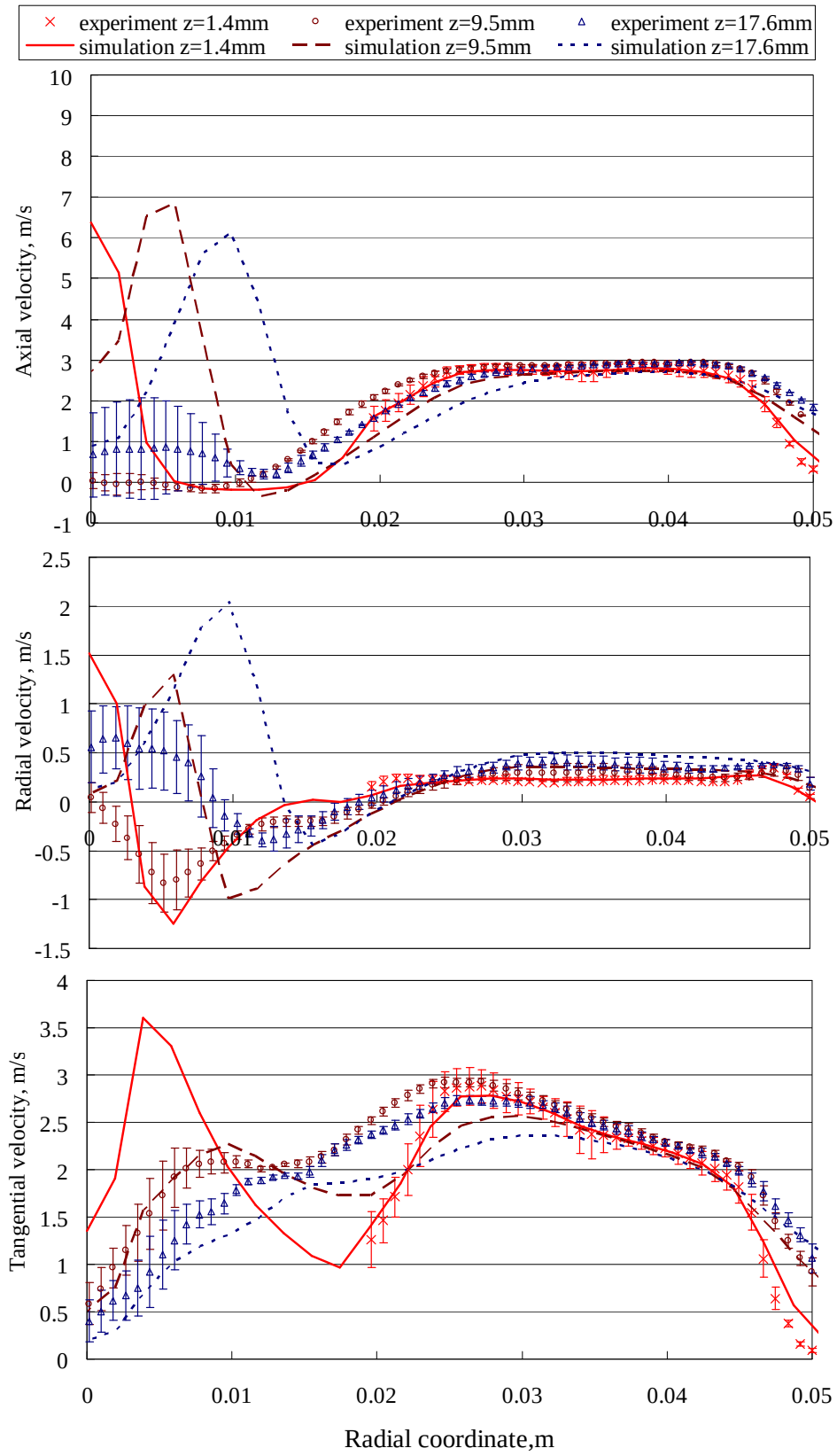

Figure 4. Predicted mean velocity components at different downstream elevations (z=1.4mm, 9.5mm and 17.6mm).

Figure 5 shows the predicted droplet number density at different downstream elevations compared with experiment. The peak points and trends are all in good agreement with the experimental data. The main difference here is that the simulation provides more droplets than the experiment, and the closer to the atomizer, the more overestimation it has. This is reasonable because accurate measurements of droplet number density in the high number density region close to the nozzle are very difficult, and that is why it is always suggested to be used in a qualitative way rather than quantitatively [2].

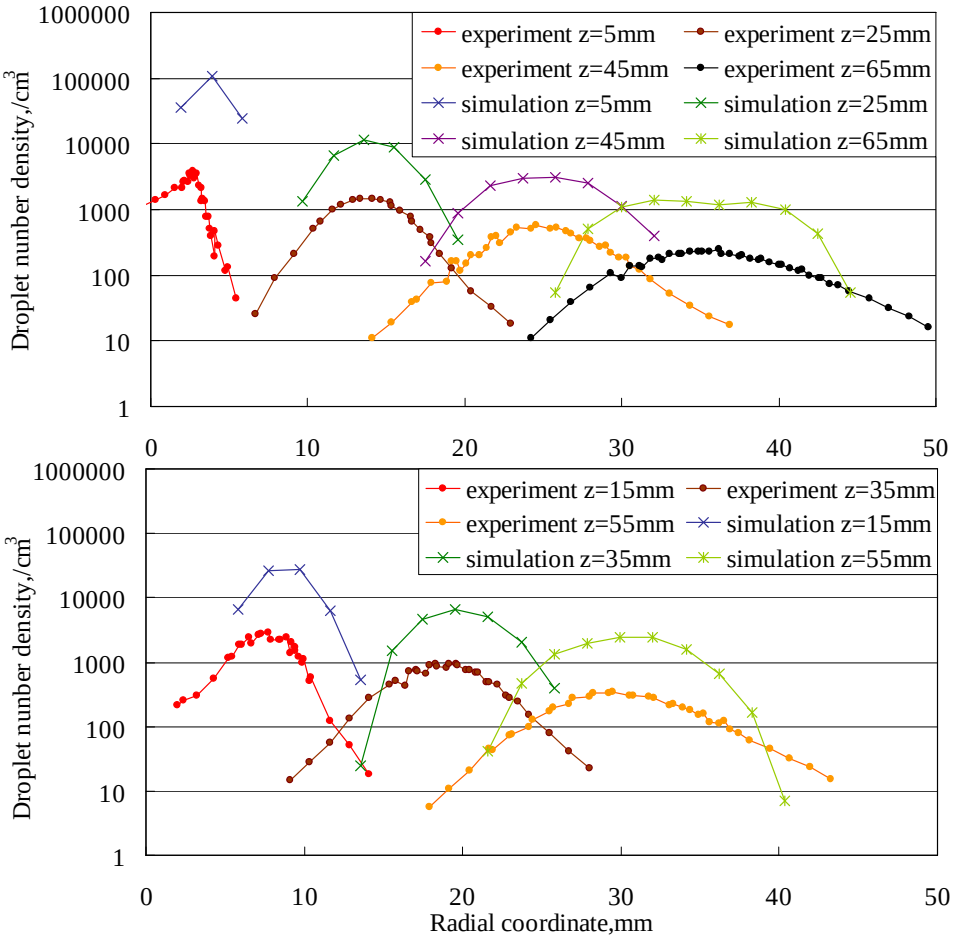

Figure 5. Predicted droplet number density at different downstream elevations.

Figure 6 shows the predicted SMD of the droplets. In consideration of the uncertainties of measurements and the calculation of SMD with the captured droplets, the predictions are pretty good. It seems that in contrast with the experiment, the simulation does not predict any SMD in the inner region of the cone, and the droplets are more narrowly distributed than in the experiment at downstream elevations close to the nozzle. One phenomenon to be noticed is that in some region where a small droplet number density exists in Figure 5, there is no droplet observed in Figure 6. It indicates that more droplets are required to be injected into the domain and sampled in order to ensure a more accurate distribution of particle diameters. Another explanation of the deviation is that in strongly non-homogeneous diffusion-dominated flows, where small particles should become uniformly distributed, the discrete random walk (DRW) model employed in the simulation may give nonphysical results and show a tendency for such particles to concentrate in low-turbulence regions instead.

The predicted mean axial and radial velocities of the droplets are shown in Figure 7. Overall they are in good agreements with the experiment while the same problem as the SMD predictions exists.

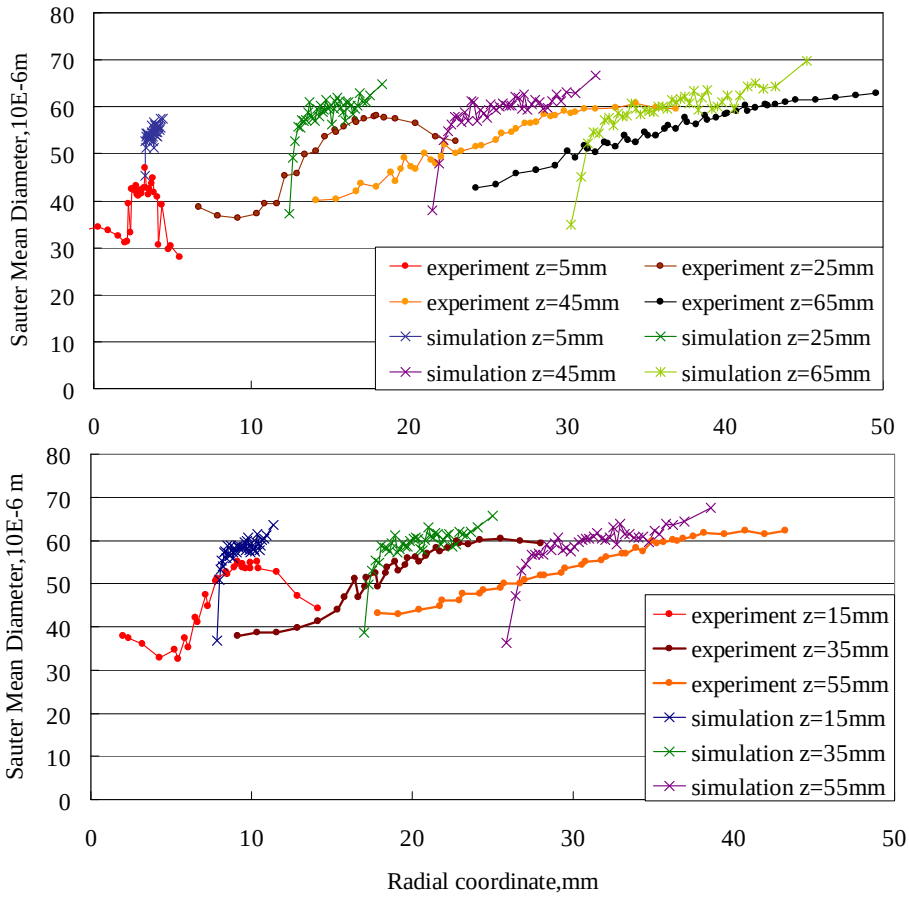

Figure 6. Predicted SMD of the droplets at different downstream elevations.

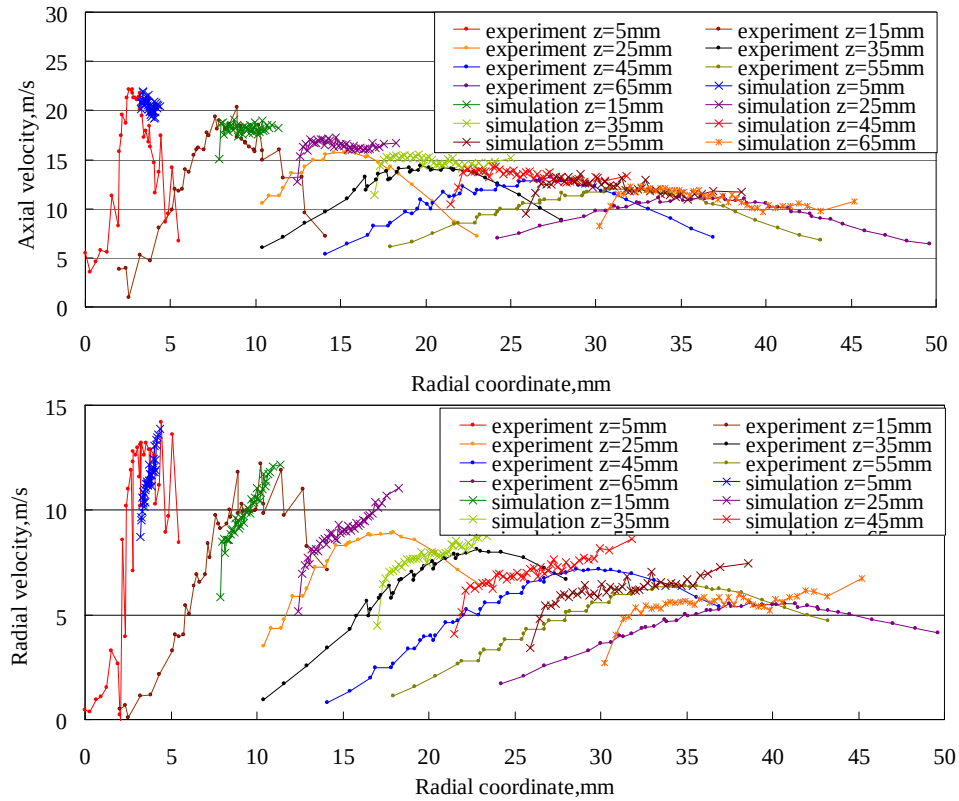

Figure 7. Predicted mean axial and radial velocities of the droplets at different downstream elevations.

The mean mixture fraction variance with and without the source term because of evaporation taken into account are compared in Figure 7. Due to the evaporation of the droplets, the peak value of mean mixture fraction variance rises from 0.013 to 0.016, and the main difference occurs at the root of the flame, where most of the evaporation takes place. This is also the same region where the scalar dissipation changes with the peak value of scalar dissipation increasing from $13\,s^{-1}$ to $17\,s^{-1}$.

With the source term of the mixture fraction variance the peak temperature is about 1860K, which is within 10K higher than without the evaporation source term and the high temperature region is a little contracted. The average temperature at the outlet remains about 700K, which is compatible with the temperature at the exhaust of 550 K in the experiment.

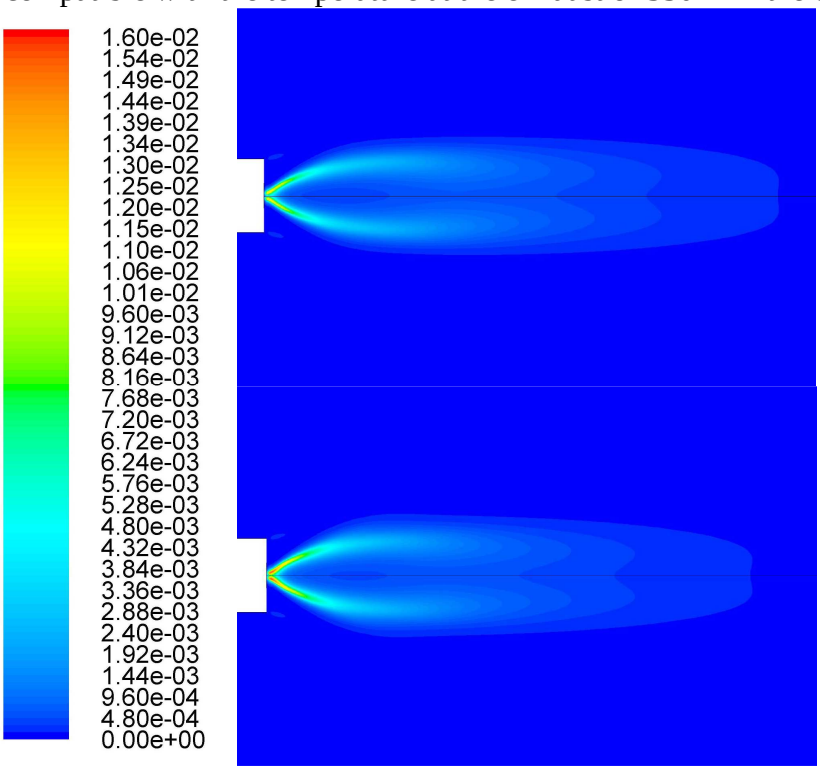

Figure 7. Comparison of mean mixture fraction variance.
(upper: without the source term due to evaporation, lower: with the source term)

Since in the NIST flame the influence of the source term on the mixture fraction variance only occurs in this lower region while the combustion mainly occurs in the flame area, the combustion characteristics are not strongly influenced by the modeling of the variance equation.

5.Conclusions

In this study, a turbulent methanol spray flame in a chamber studied experimentally at the NIST was numerically investigated and validated by the experimental data. The Euler-Lagrange method and the steady laminar flamelet model with a detailed reaction mechanism of R.P. Lindstedt and M.P. Meyer were employed. With the standard k-ε model and the enhanced wall treatment, the predicted mean velocity components of the air flow at various downstream elevations were in agreement with the experimental data. The deviations at small radii may be attributed to both numerical and experimental causes. The droplet number density, SMD, and the mean axial and radial velocities of the droplets were validated by the measured data. It seems that in the simulation the droplets were more centralized distributed than in the experiment especially when it's close to the nozzle.

In addition, the effect of the source term of the mixture fraction variance due to evaporation was also investigated numerically. The result showed that although the source term had influence on the calculation in the lower part of the flame, where the peak mean mixture fraction variance increased from 0.013 to 0.016 and the peak scalar dissipation increased from $13\ s^{-1}$ to $17\ s^{-1}$, the peak temperature increased only within 10K, and the combustion characteristics do not change much.

References

[1] Magnussen B.F., "On the structure of turbulence and a generalized eddy dissipation concept for chemical reaction in turbulent flow", *19th AIAA Meeting*, St. Louis, 1981.

[2] John F. Widmann and Cary Presser, "A benchmark experimental database for multiphase combustion model input and validation", *Combust and Flame* 129: 47–86 (2002).

[3] D. P. Schmidt, I. Nouar, P. K. Senecal, et al, "Pressure-swirl atomization in the near field", *SAE Paper 01-0496*, SAE, 1999.

[4] Crocker, D.S., Widmann, J.F., Presser, C., "CFD modeling and comparison with data from the NIST reference spray combustor", *ASME International Mechanical Engineering Congress and Exposition*, 2001.

[5] J. Collazo, J. Porteiro, D. Patiño, J.L. Miguez, E. Granada, J. Moran, "Simulation and experimental validation of a methanol burner", *Fuel* 88: 326–334 (2009).

[6] Bram de Jager, *Combustion and noise phenomena in turbulent alkane flames*, PhD thesis, Twente University, 2008.

[7] Cary Presser, "Application of a benchmark experimental database for multiphase combustion modeling", *Journal of propulsion and power, Technical Note*, 22: 1145-1148 (2006).

[8] Z. Han, S. Perrish, P. V. Farrell, and R. D. Reitz, "Modeling Atomization Processes of Pressure-Swirl Hollow-Cone Fuel Sprays", *Atomization and Sprays*, 7(6):663–684 (1997).

[9] A. H. Lefebvre, *Atomization and Sprays*, Hemisphere Publishing Corporation, 1989.

[10] C. Weber, *Zum Zerfall eines Flüssigkeitsstrahles*, ZAMM, 11:136–154 (1931).

[11] N. Dombrowski and P. C. Hooper, "The effect of ambient density or drop formation in sprays", *Chemical Engineering Science*, 17:291–305 (1962).

[12] D. P. Schmidt, M. L. Corradini, and C. J. Rutland, "A two-dimensional, non-equilibrium model of flashing nozzle flow", *3rd ASME/JSME Joint Fluids Engineering Conference*, 1999.

[13] G. I. Taylor, "The shape and acceleration of a drop in a high speed air stream", Technical report, *the Scientific Papers of G. I. Taylor, ed., G. K. Batchelor*, 1963.

[14] P. J. O'Rourke, *Collective Drop Effects on Vaporizing Liquid Sprays*, PhD thesis, Princeton University, Princeton, New Jersey, 1981.

[15] Lindstedt, R.P. and M.P. Meyer, "A dimensionally reduced reaction mechanism for methanol oxidation", *Proceedings of the Combustion Institute*, 29(1):1395-1402 (2002).

[16] C. M. Muller, H. Breitbach, and N. Peters, "Partially premixed turbulent flame propagation in jet flames", Technical report, *25th Symposium (Int) on Combustion*, The Combustion Institute, 1994.

[17] B. Binniger, M. Chan, G. Paczkko, and M. Herrmann, "Numerical simulation of turbulent partially premixed hydrogen flames with the flamelet model", Technical report, *Advanced Combustion Gmbh*, Internal Report, 1998.

[18] C.Hollmann and E.Gutheil, "Modeling of turbulent spray diffusion flames including detailed chemistry", *Twenty-sixth symposium (international) on combustion*, The combustion institute, (1996)1731-1738.